# Segmentation-Based Unsupervised Terrain Classification for Generation of Physiographic Maps

Tomasz F. Stepinski and Chaitanya Bagaria

***Abstract*—Developing an effective method for automatic mapping of physiography is of great interest because such maps have wide range of applications, but creating them manually is expensive and suffers from lack of standards. Many automapping methods have been proposed, but most yield pixel-based maps that do not quite match an appearance and usability of manually drawn maps. In this letter, we propose a method for autocreation of a physiographic map that has handmadelike appearance and functionality. The new method relies on the concept of stacked classification. First, the outcome of existing pixel-based classification is used to construct new features that contain contextual information around each pixel. Second, these new features are used by a segmentation/classification algorithm to create a final map showing generalized landform classes. We describe the design of our method and demonstrate its utility by mapping the physiography of Tharsis region on Mars. A framework of the new method is general enough to improve upon maps created by all previous pixel-based methods. Potential applications include the following: facilitating efficient geologic mapping, enabling computational comparative geomorphology, more effective visualization of topography, and fusion with other data layers within the GIS framework. The method can also be applied without modification to create segmentation-based maps of land covers.**

***Index Terms*—Classification, digital elevation model (DEM), landform, mapping, Mars, segmentation, terrain.**

## I. Introduction

THE physiographic map of a study area is the thematic map of its constituent landforms. The purpose of such a map is to visualize spatial relations between different landforms thus providing insights into geologic processes that shaped the present-day landscape of the study area. Most study areas contain several different landforms; typically, each landform is scattered among a number of disconnected surface patches. A handmade physiographic map is a mosaic of such patches where each patch is assigned a landform label on the basis of visual interpretation of an image. The slowness and expense of manual mapping calls for automation of the mapping process. Fortunately, the surface properties that distinguish between different landforms can be described quantitatively by a set of numerical measures called terrain attributes which are derived from a digital elevation model (DEM) of the surface. Thus, in principle, a computer-generated physiographic map can be obtained fast and at the minimum cost by an algorithm parsing a DEM of the study area.

Seizing this opportunity, a number of researchers had developed methods for automatic mapping of landforms. These methods can be divided into those which utilize machine learning and those which do not [1]–[4]. The machine learning-based methods can be further grouped into those [5]–[10] using unsupervised learning techniques and those [11]–[15] using supervised techniques. Moreover, all methods can be grouped into pixel-based methods [3], [5]–[13], where an algorithm assigns landform label for each pixel in a DEM separately and segmentation-based methods [1], [4], [14], [15], where an algorithm assigns landform labels for multipixel but attribute-homogeneous segments of the landscape. Different methods make use of different terrain attributes as they are designed for various purposes. In particular, Iwahashi and Pike [3] had developed an unsupervised method for classification of landforms based on only three terrain attributes: slope gradient, surface texture, and local convexity. Their pixel-based classification (hereafter referred to as IP classification) is achieved by using the nested means approach [16], [17], a nonmachine learning technique that yields a decision tree capable of mapping the three terrain attributes into statistically predefined landform labels. This simple and efficient method autogenerates physiographic maps that approximate quite well [13], [18] the maps created manually via photo interpretation.

All aforementioned methods are designed to map well-defined unmixed terrain types. This is in contrast to handmade maps featuring more generalized classes that mix simpler terrain types. In this letter, we present a method capable of mapping such generalized classes. The core idea behind our method is to utilize the concept of stacked classification [19], [20]. A stacking algorithm uses the outcome of a base classifier (designed to map simple terrain types) to construct contextual features for a secondary classifier (designed to map generalized landform classes). We use the IP classification as the base classifier and a combination of segmentation/classification algorithm as the secondary classifier.

The new method yields a physiographic map that differs from the IP map in a number of features. First, it maps generalized landform classes, more in line with what is sought by most end users. Second, the segmentation-based design of our method produces a smooth polygon-based map that is stored in the GIS-standard shapefile format. The original IP method yields a pixel-based map that has an undesirable granular appearance and needs to be stored in a raster format. Third, a rigid structure of the nested means-based decision tree utilized by the IP

Manuscript received February 26, 2009; revised April 20, 2009. This work was supported in part by the National Science Foundation under Grant IIS-0812271 and in part by NASA under Grant NNG06GE57G.

T. F. Stepinski is with the Lunar and Planetary Institute, Houston, TX 77058-1113 USA (e-mail: tom@lpi.usra.edu).

C. Bagaria is with the University of Houston, Houston, TX 77204-3010 USA (e-mail: chaitanya.bagaria@gmail.com).

Color versions of one or more of the figures in this paper are available online at http://ieeexplore.ieee.org.

Digital Object Identifier 10.1109/LGRS.2009.2024333

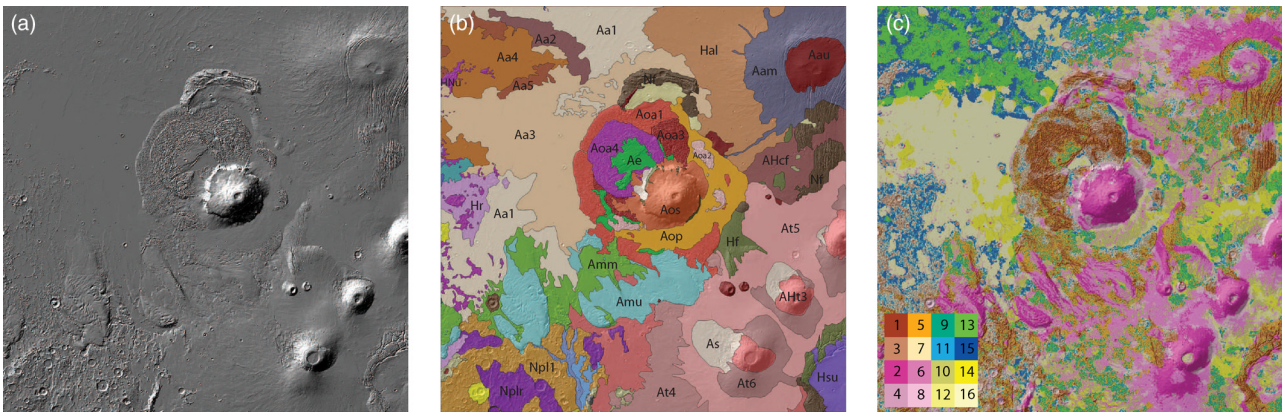


Fig. 1. Tharsis region on Mars. (a) Shaded relief. (b) Geologic map, labels [21] indicate prominent units. (c) Physiographic map obtained using Iwahashi and Pike's classification, see text for description of legend.

method restricts a number of landform classes to 8, 12, or 16, and the physical meaning of those classes is set *a priori* by statistical properties of a landscape. In the new method, the number of landform classes is a free parameter. The physical meaning of the classes is given by an analyst (if supervised classification of segments is desired) or is interpreted *a posteriori* (in case of unsupervised classification of segments). In this letter, we focus on an unsupervised variant of our method.

## II. Methodology

### A. Study Area

Our study area is the Tharsis region on planet Mars. This choice reflects our long-standing interest in Martian surface [6], [10], [14], [15], but, in addition, we want to highlight an application of automapping for planetary surfaces for which topographic data exist or is about to become available but geomorphic knowledge is lacking. The Tharsis region on Mars [Fig. 1(a)] is an enormous volcanic plateau containing a number of large volcanoes including Olympus Mons—the largest volcano in the solar system. Tarsis landscape with its many intervened landforms presents a good test case for an automapping technique. The manually drawn [21] geologic map of the region [Fig. 1(b)] contains 43 different geologic units. Note that geologic units are not the same as landform classes so the geologic map does not provide a "ground truth" against which the autogenerated map can be compared. Nevertheless, some level of correspondence between physiography and geology is expected as the geologic units are established mainly (but not exclusively) on the basis of photo interpretation of surface features. The site's center is located at about $-137^\circ$ E and $13^\circ$ N. The DEM is provided by the Mars Orbiter Laser Altimeter Mission Experiment Gridded Data Record (MEGDR) [22] and has the resolution of 128 pixels/degree. For the purpose of this letter, the MEGDR was resampled to 16 pixels/degree (or $\sim$4 km/pixel near the equator) and the $1024 \times 1024$ clip was taken to represent the study area.

### B. Base Classification

The first step is to classify each pixel in the study area into one of 16 terrain types (classes) using the Iwahashi and Pike's classifier; the result is shown in Fig. 1(c). The legend to Fig. 1(c) is organized in a square array; the top row groups classes (1,5,9,13) representing rough, convex terrain; the second row groups classes (3,7,11,15) standing for rough, concave terrain; the third row groups classes (2,6,10,14) representing smooth, convex terrain; the last row groups classes (4,8,12,16) corresponding to smooth, concave terrain. In each row, progressively larger values of labels indicate gentler terrain. The resultant map gives a good visual indication of the overall site's physiography, however zooming in reveals a granular character of the classification that stems from assigning a very specific landform label to each pixel.

### C. Secondary Features

The secondary features capture contextual information around a given pixel and are calculated from the labels (1 to 16) returned by the base classifier. The secondary features are combined into a pixel-attached feature vector which describes, in a generalized manner, surface character in the neighborhood of this pixel. We calculate 19 such features. The first 16 features are normalized frequencies of the IP labels contained within a $N \times N$ square window centered on the focus pixel. The value of $N$ controls the degree of surface generalization; results for $N = 11$ are presented in this letter. The remaining three features characterize a local pattern of labels. Two windows may have a similar frequencies but different spatial distributions of the labels. We calculate pattern features using a modification of the multiscale local binary pattern (LBP) operator originally designed [23] to measure texture in grayscale images. Our modified $LBP_{P,R}$ operator compares a label, $L_c$ of the focus pixel, with labels, $L_p$, of $P$ pixels distributed uniformly on a circle having the radius $R$ and the center located at the focus pixel

$$LBP_{P,R} = \sum_{p=1}^{P} s(L_p, L_c) 2^p \qquad (1)$$

where $s(L_p, L_c) = 1$ if $L_p \neq L_c$ and $s(L_p, L_c) = 0$ if $L_p = L_c$. The value of $LBP_{P,R} = 0$ if the entire neighborhood is assigned the same label; other values of $LBP_{P,R}$ discriminate between different patterns of "contaminant" labels. We

calculate the value of $LBP$ for ($P = 8,\ R = 1$), ($P = 16,\ R = 2$), ($P = 24,\ R = 3$); nearest-neighbor approximation is used to calculate a label of a pixel at the specified radius. The $LBP_{P,R}$ values are transformed to a set of $P + 1$ ordinal tags that correspond to rotationally invariant and "uniform" pattern-types indicating progressively larger degree of nonuniformity (see [23] for details).

Note a difference between the terrain attributes used by the IP classifier and the secondary features to be used in our classification. Whereas the first measure the surface properties directly, the second describe surface in generalized terms. For example, a 19-features vector (0.7,0,0,0,0.3,0,0,0,0,0,0,0,0,0,0,0,1,3,6) indicates that a terrain around a focus pixel is 70% steep, rough, and convex; 30% moderate, rough, and convex; the terrain is uniform on small spatial scale ($LBP_{8,1} = 1$), but become moderately contaminated (by class 5) farther from the focus pixel ($LBP_{16,2} = 3,\ LBP_{24,3} = 6$). The secondary features generalize the original geomorphic description of the surface. Partitioning a site into segments on the basis of homogeneity of secondary, rather than original geomorphic vectors leads to a physiographic map that depicts classes that consist of mixtures of landform elements that "belong" together (on the basis of similarity measure). Such a map has functionality and esthetics similar to those of handmade maps.

### D. Segmentation and Classification

We use 19-features vectors to partition the site into mutually exclusive and exhaustive segments so that each segment contains pixels having approximately uniform vectors. We also cluster these segments into a number of generic classes that are subsequently semantically interpreted. Both, segmentation and clustering are achieved *simultaneously* using the recursive hierarchical segmentation (RHSEG) algorithm [24]. The RHSEG algorithm is a hybrid of region growing and feature clustering approaches to partitioning an image or, in our case, to segmenting the landscape scene. Starting from individual pixels as regions seeds, the algorithm alternates between merging similar adjacent regions into larger regions (segmentation) and merging labels of nonadjacent similar regions (clustering). Both steps utilize a feature-based user-defined similarity criterion to decide whether to merge the segments. As this two-step process is iteratively repeated, it produces a natural hierarchy of both: spatial segmentations and clusters of features. In spatial dimension, a coarser segmentation preserves boundaries between segments in all finer segmentations. In feature space, larger clusters incorporate smaller clusters (corresponding to a more narrowly defined landform) created in previous iterations.

The RHSEG algorithm has very desirable properties for autogeneration of physiographic maps. As we have noted in the Introduction, a manual creation of a physiographic map consists of partitioning a site into surface patches and assigning landform labels to those patches. The RHSEG recreates this process in an algorithm; the segments correspond to patches and the cluster identifiers correspond to landform labels. Because the computation follows roughly the same steps as taken by an analyst, the resultant map has information esthetics similar to those found in manually drawn maps. However, whereas in manual mapping, the patches are delineated to conform to landforms types which have been selected *a priori* by an analyst, in the RHSEG-generated map landform classes (clusters) and segments are fundamentally linked as they both reflect the existing patterns in the spatial data. Thus, our automapping is an exploratory mapping—both landform types and their spatial presence are derived. This is in contrast to manual mapping that could be referred to as an exploitation mapping because it utilizes existing knowledge about landform types to assign them to different spatial locations. Stopping the RHSEG algorithm at a given iteration level results in a physiographic map of a certain geographical and feature-space resolutions; less iteration produces a map with finer resolution and more iterations produces a map with coarser resolution.

## III. Results

We have applied our method to the Tharsis region test site. The base classification was calculated using the Arc/INFO Macro Language script available as a part of [3]. The outcome of this calculation is the map shown in Fig. 1(c), where each of the 1024 × 1024 pixels is assigned one of 16 landform classes. The secondary features were calculated using a Matlab code. The final segmentation and classification was calculated using the RHSEG software [25]. Note that the RHSEG works on the same [26] principle as a popular Definiens commercial image analysis software.

The RHSEG has a number of parameters that need to be set. The most important parameter is a similarity criterion for merging regions; we have set this parameter to the "Entropy" method. The core idea behind the entropy method is to execute mergers that minimize the change of entropy. The entropy $H$ of a region $X$ is defined as an entropy of its mean feature vector; i.e., $n \sum f_i \log f_i$, where $n$ is the number of pixels in a region and $f_i$ is the regional mean of the $i$th component of the feature vector. The summation extends over all dimension of the vector ($i = 1, \ldots, 19$ in our case). The RHSEG calculates $\Delta H = H(X_1 + X_2) - H(X_1) - H(X_2)$ between the pairs of adjacent (segmentation step) and nonadjacent (clustering step) regions and the pairs of regions with the smallest value of $\Delta H$ are merged. Another important parameter governs a depth of segmentation hierarchy saved for future analysis. Keeping the results of all iterations is neither feasible nor necessary. We set this parameter so the RHSEG starts saving the segmentation results when the feature vectors are already clustered into 20 landform classes (there are much more segments present at that stage as multiple segments corresponds to a single class). The most-detailed retained partitioning is referred to as level 0 segmentation. Subsequent, progressively coarser segmentations are referred to as level $1, \ldots, 19$, respectively.

Fig. 2 shows the level 11 segmentation consisting of 2382 segments grouped into nine landform classes. The legend to Fig. 2 lists the nine classes; each class is assigned a color and a numerical label (as set by the RHSEG). A "composition" of each class in terms of IP terrain types is given by a pie graph. Our rough interpretation of each class, in terms of terrain texture, convexity, and slope, is given by pictorial symbols. For example, landform labeled 1024 is interpreted as steep convex

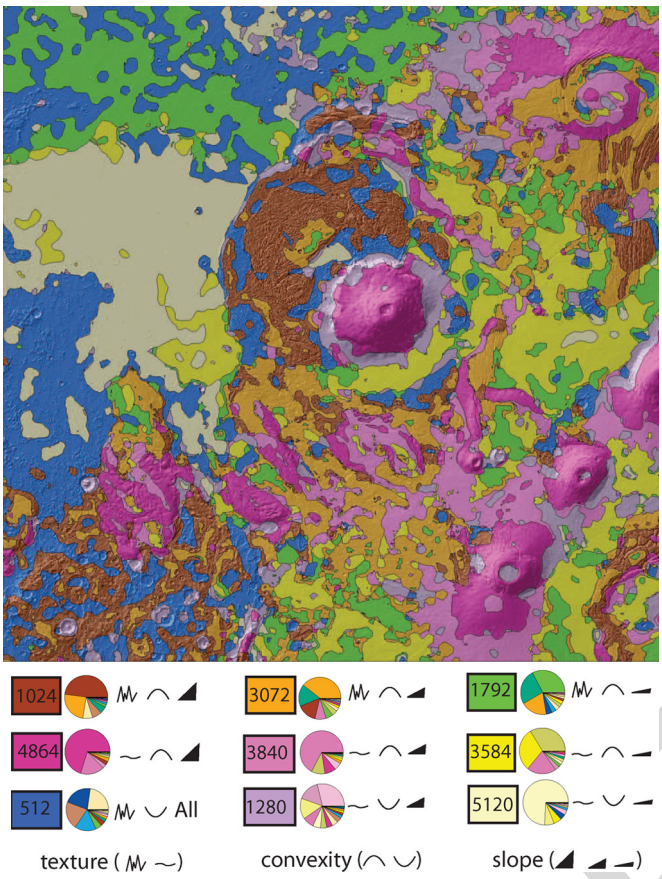


Fig. 2. Autogenerated physiographic map of Tharsis region on Mars. Numbers in a legend are numerical labels assigned to the landform classes by the RHSEG algorithm. Pie graphs show composition of classes in terms of the IP terrain types. Symbols represent our interpretation of the landform classes in terms of texture, convexity, and slope.

terrain characterized by rough surface (fine texture). Note that RHSEG-generated classes vary in their correspondence to the IP terrain types. For example, ∼50% of pixels contained in the aforementioned class 1024 belong to IP terrain type 1, ∼25% belong to terrain type 5, and the remaining ∼25% belong to other terrain types. Thus, our interpretation of class 1024 is a shortcut; a more detailed narrative may be required. Most classes are heavily dominated by a single IP terrain type (class 4864 by type 2, class 3840 by type 6, class 5120 by type 16), but some (512, 1792) are not. The colors depicting the classes in Fig. 2 were chosen to correspond to their dominant terrain type if possible. This is why the maps on Figs. 1(c) and 2 have similar colors.

Notwithstanding visual similarity (which decreases with increased magnification), the map created by our method is quite different from the map [Fig. 1(c)] created using the IP method. Generalized classes summarize the geomorphic setting of the test site in a clearer and more straightforward fashion making the map more useful to end users. There is a computational cost associated with this improvement; the IP classification takes only minutes to compute, the RHSEG takes 7 h to segment the test site using 2.0-GHz Intel processor. Comparison of our physiographic map to the geologic map [Fig. 1(b)] shows some correspondence between spatial distribution of landform classes and geologic units. Note that the geologic map is manually drawn using both objective criteria (such as, surface morphology and its age) and subjective criteria (such as, nomenclature, history of previous investigations, etc.). For example, the unit AHt3 is defined [21] as "...large volcanic shields and associated lava flows of Arsia Mons, Pavonis Mons, and Ascraeus Mons," whereas the unit Aos is defined as "... young lava flows associate with Olympus Mons." Both units refer to the same landform (as correctly indicated by the map on Fig. 2), different geologic labels stem from different geographic location. Thus, closer correspondence between physiographic and geologic map cannot be expected. The autogenerated physiographic map provides an objective geomorphic information to be utilized for creation of geologic map.

## IV. Summary and Conclusion

In this letter, we have proposed a method for autogeneration of a physiographic map from a DEM. Our method fuses two existing techniques, classification of pixels into terrain types and the RHSEG algorithm for image segmentation/classification, to generate segmentation-based, visually esthetic and ready-for-analysis map generalized landform classes. The framework of our method allows for use of any base classifier (for example, for classifiers proposed in [2], [8]), but in this letter, we have focused on the IP classifier that uses texture, convexity, and slope as terrain attributes. Consequently, generated maps depict landform classes abstracting landforms on the basis of these three attributes. Because our method relies on unsupervised classification each class needs to be postinterpreted; however, such an interpretation is easily obtained from terrain types making up each class.

The power of automapping comes from its ability to map many sites efficiently to the same standards. With such applications in mind, the following considerations should be taken into account. The IP base classifier uses statistical distributions of terrain attributes to categorize pixels. Thus, meaning of terrain types is relative to a site; for example, the terrain type 1 in one site may not have the same absolute values of terrain attributes as the terrain type 1 in another site. If it is desirable to preclassify sites with terrain types having the same absolute meaning, a base classifier should be used on concatenation of pixels from all the sites. Moreover, because the RHSEG yields landform classes via clustering, the precise meaning of classes is unique to each site. If it is desirable to have uniform meaning of landform classes throughout a series of sites, the segments in a selected site should be treated as a training set, and the segments in all other sites should be labeled using a supervised classification technique [27].

The maps generated by our method are more useful to end users than the maps depicting unmixed terrain types [2], [3], [8] because they partition the site in a fashion similar to what an analyst would do manually. The map can be stored in the standard ArcGIS shapefile format to be used in further analyses when combined with other layers of data. For example, combining a physiographic map of a given (terrestrial) site with a land cover map of the same site would facilitate a quantitative analysis of dependence of land cover on landform class. Similar examples abound. The difference between our method and previously

published [1], [4] segmentation-based mapping methods is an unsupervised approach to classification of landforms. In [1] and [4], the Definiens (previously eCognition) software was used to first segment a site and than classify the segments using a predefined classification scheme. In contrast, our method is a two-step approach wherein predefined terrain types are assigned by a base classification scheme, but landform classes arise from clustering of segments.

We envision several applications for our method. First application is to expedite creation of geologic maps in planetary science context where surfaces are still being explored and the manual analysis does not keep up with availability of new data. Second application is for quantitative comparative geomorphology where our automapping facilitates numerical comparison between composition of landform classes in different sites. Third application is for visualization; draping our physiographic map over the shaded relief (see Fig. 2) creates a "topo-thematic" map wherein relief is communicated by a hillshade and geomorphology is communicated by the legend to the physiographic map. This is particularly useful for visualizing large sites (like the Tharsis region) where terrain attributes such as texture, convexity, or even slope are not conveyed well by shaded relief. Shaded relief gives an overall impression about the character of the surface [see Fig. 1(a)], but a topo-thematic map of the same size (see Fig. 2) gives much more detailed account.

Finally, we notice that the idea of using the principle of stacked classification in order to generate better maps is not restricted to physiography. The same method can be used to generated segment-based maps of land cover from existing pixel-based data. Moreover, the results of base classification of terrain types and land cover can be fused to form secondary features that describe broader character of the site. The segmentation/classification step of our method will yield a map with classes that abstract physiography-land-cover instances [28].

## ACKNOWLEDGMENT

A portion of this letter was conducted at the Lunar and Planetary Institute, which is operated by the USRA under Contract CAN-NCC5-679 with NASA. This is LPI Contribution 1484.

## REFERENCES

[1] L. Dragut and T. Blaschke, "Automated classification of landform elements using object-based image analysis," *Geomorphology*, vol. 81, no. 3/4, pp. 330–344, Nov. 2006.

[2] A. L. Gallant, D. D. Brown, and R. M. Hoffer, "Automated mapping of Hammond's landforms," *IEEE Geosci. Remote Sens. Lett.*, vol. 2, no. 4, pp. 384–388, Oct. 2005.

[3] J. Iwahashi and R. J. Pike, "Automated classifications of topography from DEMs by an unsupervised nested-means algorithm and a three-part geometric signature," *Geomorphology*, vol. 86, no. 3/4, pp. 409–440, May 2007.

[4] S. van Asselen and A. C. Seijmonsbergen, "Expert-driven semi-automated geomorphological mapping for a mountainous area using a laser DTM," *Geomorphology*, vol. 78, no. 3/4, pp. 309–320, Aug. 2006.

[5] A. O. Adediran, I. Parcharidis, M. Poscolieri, and K. Pavlopoulos, "Computer-assisted discrimination of morphological units on north-central Crete (Greece) by applying multivariate statistics to local relief gradients," *Geomorphology*, vol. 58, no. 1–4, pp. 357–370, Mar. 2004.

[6] B. D. Bue and T. F. Stepinski, "Automated classification of landforms on Mars," *Comput. Geosci.*, vol. 32, no. 5, pp. 604–614, Jun. 2006.

[7] P. A. Burrough, P. F. M. van Gaans, and R. A. MacMillan, "High-resolution landform classification using fuzzy k-means," *Fuzzy Sets Syst.*, vol. 113, no. 1, pp. 37–52, Jul. 2000.

[8] A. H. Ehsani and F. Quiel, "Geomorphometric feature analysis using morphometric parameterization and artificial neural networks," *Geomorphology*, vol. 99, no. 1–4, pp. 1–12, Jul. 2008.

[9] B. J. Irvin, S. J. Ventura, and B. K. Slater, "Fuzzy and isodata classification of landform elements from digital terrain data in Pleasant Valley, Wisconsin," *Geoderma*, vol. 77, no. 2–4, pp. 137–154, Jun. 1997.

[10] T. Stepinski and R. Vilalta, "Digital topography models for Martian surfaces," *IEEE Geosci. Remote Sens. Lett.*, vol. 2, no. 3, pp. 260–264, Jul. 2005.

[11] D. G. Brown, D. P. Lusch, and K. A. Duda, "Supervised classification of types of glaciated landscapes using digital elevation data," *Geomorphology*, vol. 21, no. 3/4, pp. 233–250, Jan. 1998.

[12] T. Hengl and D. G. Rossiter, "Supervised landform classification to enhance and replace photo-interpretation in semi-detailed soil survey," *Soil Sci. Soc. Am. J.*, vol. 67, pp. 1810–1822, 2003.

[13] O. Prima, A. Echigo, R. Yokoyama, and T. Yoshida, "Supervised landform classification of northeast Honshu from DEM-derived thematic maps," *Geomorphology*, vol. 78, no. 3/4, pp. 373–386, Aug. 2006.

[14] T. F. Stepinski, S. Ghosh, and R. Vilalta, "Automatic recognition of landforms on Mars using terrain segmentation and classification," in *Proc. 9th Int. Conf. Discov. Sci.*, 2006, vol. 4265, Lecture Notes in Computer Science, pp. 255–266.

[15] T. F. Stepinski, S. Ghosh, and R. Vilalta, "Machine learning for automatic mapping of planetary surfaces," in *Proc. 19th Innov. Appl. Artif. Intell. Conf.* W. Cheetham and M. Goker, Eds., 2007, pp. 7–18.

[16] D. Guo, D. Peuguet, and M. Gahegan, "ICEAGE: Interactive clustering and exploration of large and high-dimensional geodata," *Geoinformatica*, vol. 7, no. 3, pp. 229–253, Sep. 2003.

[17] M. W. Scripter, "Nested-means map classes for statistical maps," *Ann. Assoc. Am. Geogr.*, vol. 60, pp. 385–393, 1970.

[18] J. Iwahashi, "Development of landform classification using the digital elevation model," *Ann. Disaster Prev. Res. Inst., Kyoto Univ.*, vol. 37, no. B-1, pp. 141–156, 1994.

[19] K. M. Ting and I. H. Witten, "Issues in stacked generalization," *J. Artif. Intell. Res.*, vol. 10, pp. 271–289, 1999.

[20] D. H. Wolpert, "Stacked generalization," *Neural Netw.*, vol. 5, no. 2, pp. 241–260, 1992.

[21] D. H. Scott and K. L. Tanaka, "Geologic map of the western equatorial regions of Mars," U.S. Geol. Surv. Inv. Series Map I-1802 A, 1986.

[22] D. Smith, G. Neumann, R. Arvidson, E. Guinness, and S. Slavney, "Mars Global Surveyor laser altimeter mission experiment gridded data record," NASA Planetary Data System, 2003, MGS-M-MOLA-5-MEGDR-L3-V1.0 .

[23] T. Ojala, M. Pietikainen, and T. Maenpaa, "Multiresolution gray-scale and rotation invariant texture classification with local binary patterns," *IEEE Trans. Pattern Anal. Mach. Intell.*, vol. 24, no. 7, pp. 971–987, Jul. 2002.

[24] J. C. Tilton, "Method for recursive hierarchical segmentation by region growing and spectral clustering with a natural convergence criterion," Disclosure of Invention and New Technology: NASA Case GSC 14,328-1, 2000.

[25] RHSEG, Recursive Hierarchical Segmentation (RHSEG) Pre-Processings Software, 2009. [Online]. Available: http://techtransfer.gsfc.nasa.gov/rhseg/index.html

[26] M. Baatz, G. Binnig, P. Eschenbacher, A. Melchinger, and M. Sogtrop, "Method of iterative segmentation of a digital picture," U.S. Patent 6 832 002, Dec. 14, 2004.

[27] I. H. Witten and E. Frank, *Data Mining: Practical Machine Learning Tools and Techniques*., 2nd ed. San Francisco, CA: Morgan Kaufmann, 2005, ser. Morgan Kaufmann Series in Data Management Systems.

[28] A. H. Ehsani and F. Quiel, "A semi-automatic method for analysis of landscape elements using shuttle radar topography mission and Landsat ETM+ data," *Comput. Geosci.*, vol. 35, no. 2, pp. 373–389, Feb. 2009.